Axis Ratio and Raindrops Shape

The axis ratio of a particle or a raindrop refers to the ratio of its major axis to its minor axis. It can provide a measure of how elongated or flattened the droplet is.

Understanding the shapes of raindrops is important for various applications including weather forecasting, radar observations, and remote sensing of precipitation. Different raindrop shapes can affect how they interact with electromagnetic radiation, influencing radar measurements and rainfall estimates.

Raindrops are typically not perfect spheres due to various factors such as air resistance, collision with other droplets, and evaporation. They are modeled as spheroidal, also known as a rotational ellipsoid 'oblate' or 'prolate'.

Oblate raindrops are flattened or disc-like in shape. This shape occurs when the force of air resistance exceeds the gravitational force acting on the droplet, causing it to flatten as it falls through the atmosphere. Oblate raindrops are more common at lower altitudes where air density is higher and air resistance is stronger.

Prolate raindrops are elongated or cigar-shaped in appearance. This shape occurs when the droplet experiences a rapid acceleration due to strong updrafts or turbulence within a cloud. As the droplet accelerates upwards, it stretches along its axis, resulting in a prolate shape. Prolate raindrops are more commonly observed in thunderstorms or convective clouds where strong vertical motions are present.

If the ellipse is rotated about its major axis, the result is a prolate spheroid. If the ellipse is rotated about its minor axis, the result is an oblate spheroid. If the generating ellipse is a circle, the result is a sphere.

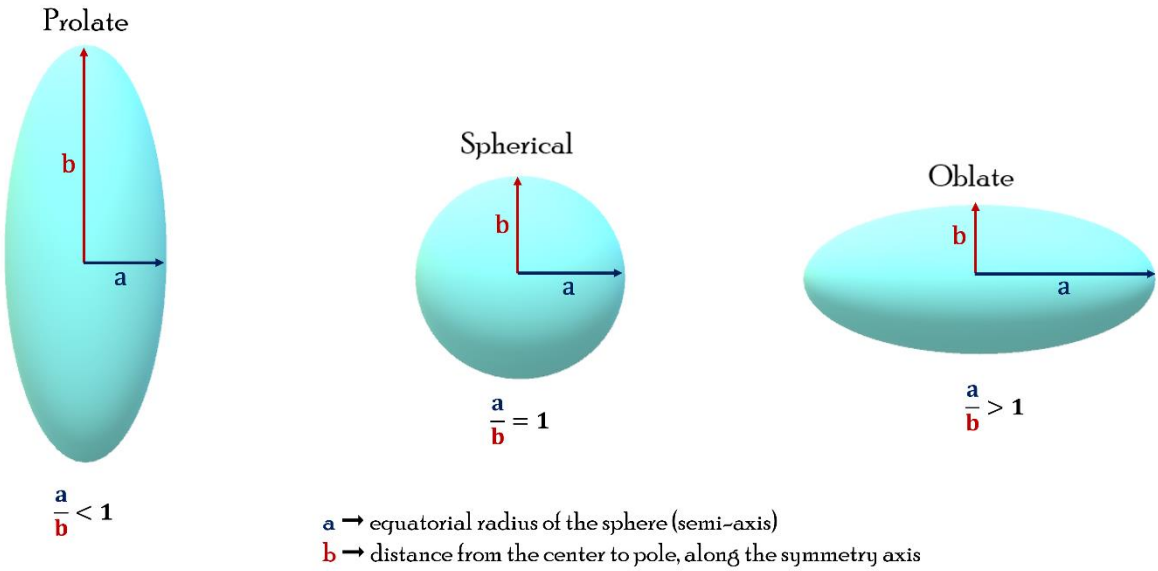

The axis ratio, along with the oblate or prolate shape of raindrops, influences how they scatter light and interact with electromagnetic radiation.

Axis Ratio parametrization

Axis ratio depends on the size of the particle/ raindrop. There are several parametrizations. We use the one below, from Mishchenko, 1999 (Chapter 16 and Chapter 3 B. IV).

$$\frac{b}{a} = 1.01668 - 0.098055D - 2.52686D^2 + 3.75061D^3 - 1.68692D^4. \quad (18)$$

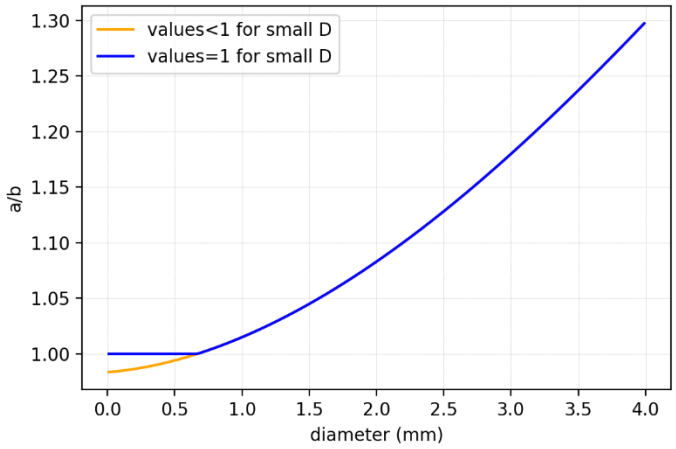

Figure 1 Axis ratio as a function of diameters D of raindrops

This parametrization results to axis ratio less than 1 for small droplets. We set axis ratio = 1 for those small droplets to ensure that they behave like perfect spheres and result to zero reflectivity.

Practically, changing the axis ratio is like changing the canting of the droplets.

Raindrop Size Distribution

The gamma distribution is a widely accepted and practical way to represent drop size distributions in precipitation research and radar meteorology.

$$N(D) = N_0 D^{\mu} \exp\{-\Lambda D\} \; [mm^{-1}m^{-3}]$$

D [mm] is the equivalent spherical drop diameter, μ is the dimensionless shape parameter which can have any negative or positive value, N_0 [$mm^{-1-\mu}m^{-3}$] is the number concentration parameter and Λ [mm^{-1}] is the slope parameter.

The three parameters (N_0, μ, Λ) of the gamma distribution enable a wide range of rainfall situations to be described. For Λ applies $\Lambda=(4+\mu)/D_m$, where D_m [mm] is the mass-weighted mean diameter, also denoted as mean volume diameter in different expressions (Testud et al. 2001).

$$D_m = \frac{(4+\mu)}{\Lambda}$$

If we use N_0=8 10^3 m^{-4}, μ=0, Λ=1.835 mm^{-1} that describes the original exponential Marshall–Palmer model \cite{M-P:5}.

In Figure 2 we see an example of M-P distribution

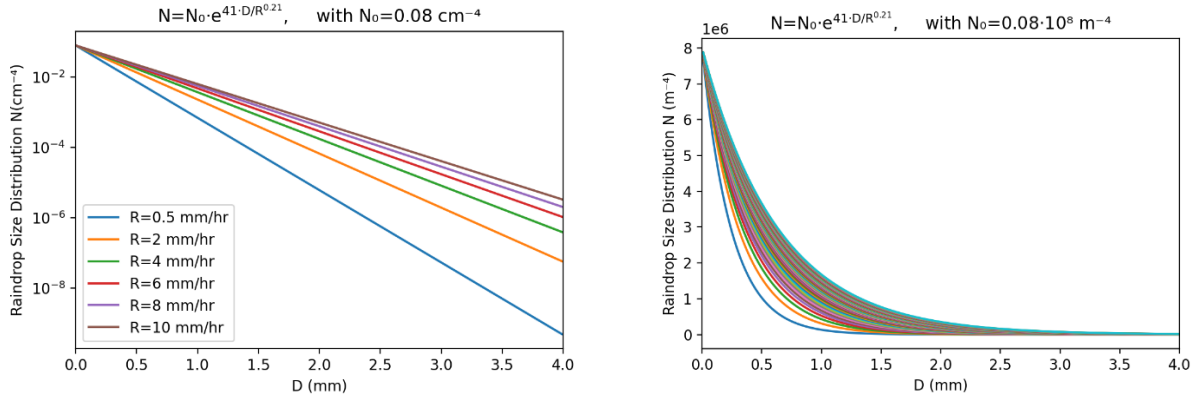

Figure 2 Marshall-Palmer Raindrop Size Distribution N as a function of diameters D In linear (left) and log (right) scale.

Some people instead of D_m, use D_o.

D_m is the mass weighted mean diameter.
D_0 is the median volume diameter, is separating the distribution in 2 parts with equal volumes.

Using the expression from Lhermitte we get the n-moment of Γ distribution:

$$\int [\exp(-\Lambda D) \cdot D^{\mu+n} dD] = \Gamma(n+\mu+1)/\Lambda^{n+\mu+1}$$

$$D_m = \frac{M_4}{M_3} = \frac{\frac{\Gamma(4+\mu+1)}{\Lambda^{4+\mu+1}}}{\frac{\Gamma(3+\mu+1)}{\Lambda^{3+\mu+1}}} = \frac{\frac{\Gamma(5+\mu)}{\Lambda^{5+\mu}}}{\frac{\Gamma(4+\mu)}{\Lambda^{4+\mu}}} = \frac{\Gamma(5+\mu)}{\Gamma(4+\mu)}\Lambda^{-1} = \frac{(5+\mu-1)!}{(4+\mu-1)!}\Lambda^{-1} = \frac{4+\mu}{\Lambda}$$

$$\Gamma(n) = (n-1)!$$

D_m is the 4th moment divided by the 3rd moment, but you have the formula to compute every moment. 4th moment means n=4, that is equal to $\Gamma(5)/\Lambda^5$, everything divided by $\Gamma(4)/\Lambda^4$. The result is $\Gamma(5)/\Gamma(4)/\Lambda$. Λ is the characteristic parameter of the exponential. Λ can be deriver as a function of D_m.

Orientation Distribution functions

An Orientation Distribution Function (ODF) is a mathematical function that describes the distribution of particle orientations relative to the incident electromagnetic field. By setting an

ODF in T-matrix calculations, we simulate how particles are oriented in space and how their orientations affect their scattering properties.

If we do not specify an ODF, we assume that the raindrops are perfectly oriented. This means that all particles are assumed to be uniformly aligned in a specific orientation relative to the incident electromagnetic field. This way, the computational model is simplified and the interpretation of the results is easier. However, this assumption does not accurately represent the real scattering scenario of droplets.

Common orientation distribution functions used in T-matrix calculations include:

Gaussian Distribution: Particle orientations follow a Gaussian or normal distribution.

This formula describes the probability density of obtaining a particular orientation angle x relative to the mean μ in a Gaussian distribution.

$$f(x) = \frac{1}{\sqrt{2\pi}\sigma} \exp\left(-\frac{(x-\mu)^2}{2\sigma^2}\right)$$

x : the orientation angle
μ : mean or average orientation.
σ : the standard deviation, which determines the spread or dispersion of the distribution.

In pytmatrix, we specify the standard deviation σ of the angle with respect to vertical orientation (this is often called the **canting angle**).

Uniform Distribution: All particle orientations are equally likely within a specified range of angles. This assumes random particle orientations with no preferred orientation.

The PDF of a uniform distribution over the interval [a,b] is given by:

$$f(x) = \frac{1}{b-a}$$

a : minimum angle
b :maximum angle
x : the orientation angle

The Uniform ODF represents a scenario where particle orientations are uniformly distributed within a specified range of angles. This means that all orientations within the specified range are equally likely to occur.

For example, if we specify a Uniform ODF over the interval [0,π], it means that particle orientations are uniformly distributed between 0 and π radians (or 0 and 180 degrees). In this case, any

orientation angle within that interval is equally likely to occur, representing a scenario where particles have random orientations within the specified range.

Further discussion and detailed analysis of the ODFs, along with the simulated measurements, will be presented in the next section.

T-matrix Scattering code

The T-matrix method is a mathematical technique used to calculate the scattering properties of particles, such as raindrops, ice crystals, or other atmospheric targets, when they interact with electromagnetic radiation. Based on solving Maxwell's equations, T-matrix method determines how electromagnetic waves interact with particles of various shapes and sizes. Overall, the T-matrix represents the scattering properties of a particle in terms of its size, shape, orientation, and material properties. It is a matrix that relates the incident and scattered electromagnetic fields and contains information about the scattering amplitude and phase.

We can use the T-matrix method to simulate and predict various radar parameters such as radar reflectivity, cross-section and polarization properties. By inputting the properties of the atmospheric particles (e.g., size distribution, shape, orientation) into the T-matrix calculations, we can simulate how these particles scatter radar signals. These simulations can be validated and compared with observed radar data.

For our study, we use the Pytmatrix (Jussi Leinonen), a valuable Python package for performing T-matrix calculations and simulating the scattering properties of particles in atmospheric science and remote sensing research (Leinonen, 2014). An example of how the class "scatterer" is calculated in Python environment can be found below.

```
scatterer = Scatterer(radius=1, wavelength=3.18, m=complex(3.128, 1.75) , axis_ratio=1,
                      thet0=45, thet=135, phi0=180, phi=0)
scat_dif_phase = radar.delta_hv(scatterer)
```

Subsequently the scattering differential phase is calculated by calling the right method of the "radar" module. More information about this package and the implemented geometry can be found in the next part and at the following link: https://github.com/jleinonen/pytmatrix/wiki

The **phase matrix S** is a complex matrix that characterizes how electromagnetic waves interact with particles and how they are scattered in different directions and polarizations. It contains information about the amplitude and phase of the scattered electromagnetic field for different scattering angles and polarizations.

$$S = \begin{pmatrix} S_{11} & S_{12} \\ S_{21} & S_{22} \end{pmatrix}$$

The **phase matrix Z** (or scattering matrix) represents the linear transformation that relates the incident electromagnetic field to the scattered electromagnetic field by a particle. It is a complex

matrix that depends on various factors including the size, shape, orientation, and material properties of the scattering particle, as well as the wavelength and polarization of the incident electromagnetic radiation.

$$Z = \begin{pmatrix} Z_{11} & Z_{12} \\ Z_{21} & Z_{22} \end{pmatrix}$$

The Z and S matrix can be 2×2 for scalar scattering (when polarization effects are not considered) or as a 4×4 matrix for vector scattering (when polarization effects are considered). The elements of each matrix correspond to:

11 the amplitude of the incident wave that is scattered into the same direction (co-polarized component)
12 »»»»»»» into the orthogonal direction (cross-polarized component)
21 »»»»»»» cross-polarized to co-polarized component
22 »»»»»»» co-polarized to co-polarized component

The **identity matrix I**, often denoted as I, is a special square matrix in linear algebra that has ones on the diagonal and zeros elsewhere. It is called the "identity" matrix because it behaves similarly to the identity element in multiplication, meaning that when it is multiplied by another matrix, the result is the same matrix.

The Z-matrix is related to the phase matrix (S) through the T-matrix (T) according to the equation:

$$Z=I+2T$$

Geometry of Ground Based Radar Observations

In order to produce simulations of radar measurements by using Pytmatrix, we have to specify the geometry of the radar beam relative to the scattering particles. This includes parameters such as the incident angle (the angle at which the radar beam strikes the particles) and the azimuth angle (the horizontal angle of the radar beam relative to a reference direction).

Specifically, we have to define the variables thet0, thet, phi0, phi.

thet0 ➞ The zenith angle of the incident beam. default =90°
thet ➞ The zenith angle of the scattered beam. default=90°
phi0 ➞ The azimuth angle of the incident beam. default=0°
phi ➞ The azimuth angle of the scattered beam. default=180°

1) Horizontally pointing radar at Backscattering Alignment (BSA) – The default of Pytmatrix They are commonly used for weather surveillance and monitoring, such as detecting precipitation, measuring rainfall rates, identifying severe weather phenomena and tracking the movement of weather systems.

ZENITH:

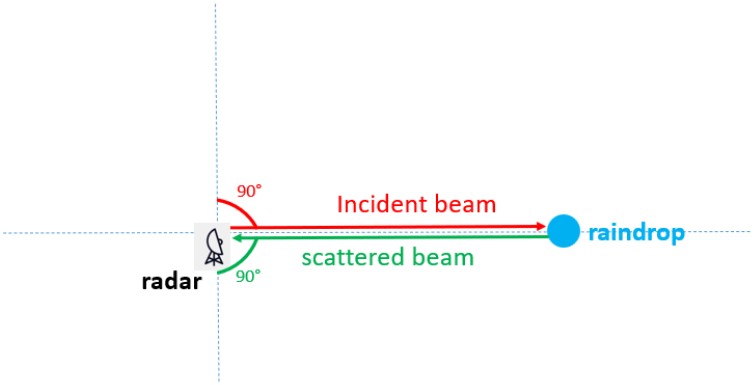

zenith angle of the incident beam: 90° (***thet0***)
zenith angle of the scattered beam: 90° (***thet***)

AZIMUTH:

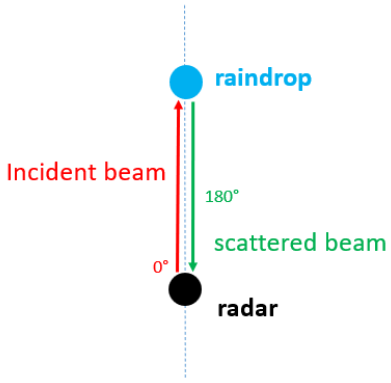

azimuth angle of the incident beam: 0° (***phi0***)
azimuth angle of the scattered beam: 180° (***phi***)

2) Vertically pointing radar at BSA

Used in research applications such as studying cloud and precipitation processes.

ZENITH:

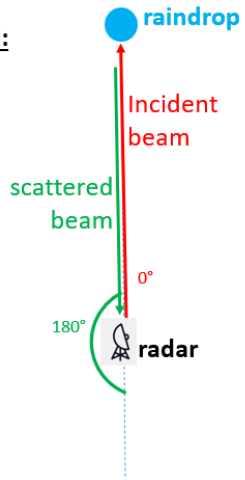

zenith angle of the incident beam: 0° (***thet0***)
zenith angle of the scattered beam: 180° (***thet***)

AZIMUTH:

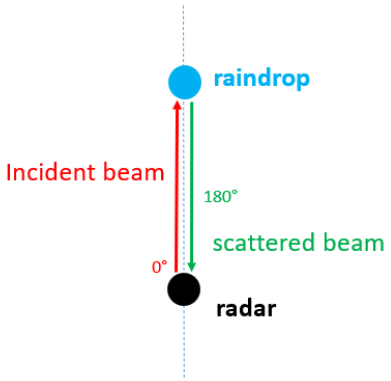

azimuth angle of the incident beam: 0° (***phi0***)
azimuth angle of the scattered beam: 180° (***phi***)

3) Radar pointing at 45° at BSA

When a radar points at an angle other than horizontal or vertical, it can affect the polarimetry and Doppler measurements.

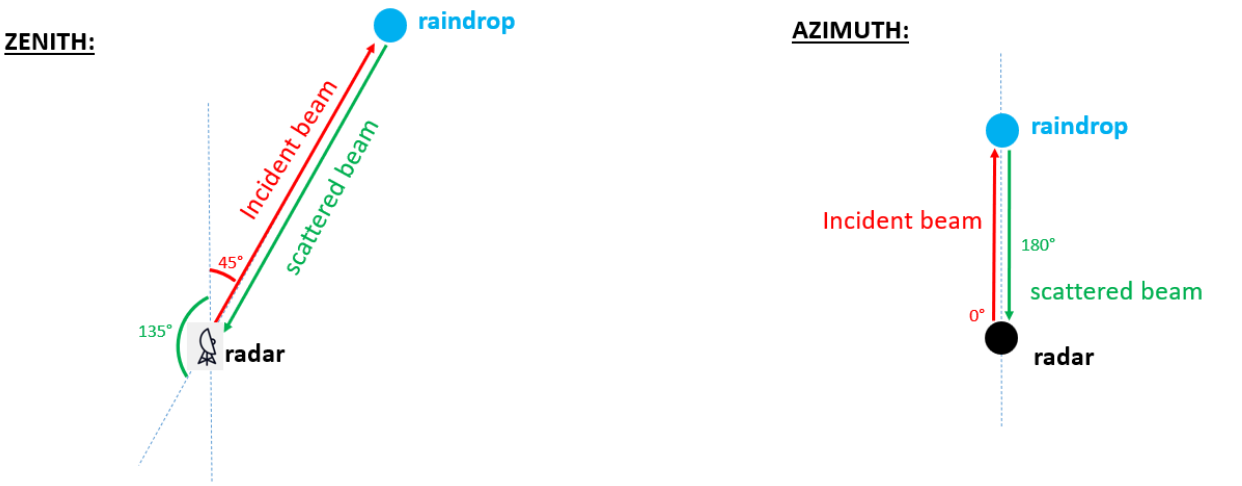

zenith angle of the incident beam: 45° (***thet0***)
zenith angle of the scattered beam: 135° (***thet***)

azimuth angle of the incident beam: 0° (***phi0***)
azimuth angle of the scattered beam: 180° (***phi***)

Single scattering Calculation for Single particles

BSA

Zij (D) elements of T-matrix (see section 2.1) are calculated for each diameter, hereafter denoted as Zij. There are several backscattering quantities we use:

• Backscattering cross sections for V-polarized and H-polarized radiation:

σ_{VV} (D) = $2\pi(Z_{11} + Z_{12} + Z_{21} + Z_{22})$ [mm^2]
σ_{HH} (D) = $2\pi(Z_{11} - Z_{12} - Z_{21} + Z_{22})$ [mm^2]

• Differential reflectivity

$Z_{DR}(D) = \sigma_{HH}(D)/\sigma_{VV}(D)$ [dB]

• Linear Depolarization Ratio

$$LDRv\ (D) = \frac{\sigma_{hv}}{\sigma_{vv}} = \frac{Z_{11}+Z_{12}-Z_{21}-Z_{22}}{Z_{11}+Z_{12}+Z_{21}+Z_{22}}\ \ (dB)$$

$$LDRh\ (D) = \frac{\sigma_{vh}}{\sigma_{hh}} = \frac{Z_{11}-Z_{12}+Z_{21}-Z_{22}}{Z_{11}-Z_{12}-Z_{21}+Z_{22}}\ \ (dB)$$

• Copolar correlation coefficient

$$\rho_{HV}(D) = \frac{\sqrt{(Z33 + Z44)2 + (Z43 - Z34)2}}{\sqrt{(Z11 - Z12 - Z21 + Z22)(Z11 + Z12 + Z21 + Z22)}}$$

• Differential Phase

δ_{HV} (D) = arctan [(Z_{43} − Z_{34})/(Z_{33} + Z_{44})]

Some T-matrix results for different drops orientation conditions are displayed in Fig. 3.

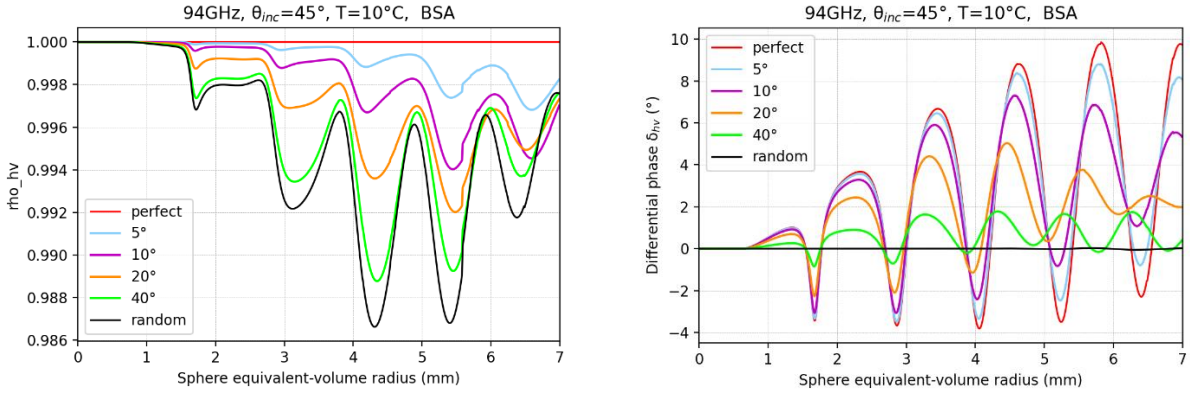

Figure 3 Co-polar correlation coefficient (rho_hv) and scattering differential phase as function of drops diameters for different orientation distribution functions.

Figure 3: Results from T-matrix method: Zij elements are calculated for a 94 GHz radar pointing at 45° and the complex refractive index of water is set at 10 °C temperature according to (Lhermitte, 1990).

The **copolar correlation coefficient (ρ_{HV})** quantifies the similarity between the horizontally and vertically polarized components of the radar signal. In Fig. 3 left, perfectly oriented drops (red line) have ρ_{HV} =1, indicating that the radar return has maintained its polarization state. On the other hand, rain drops with orientation or tilt of the drop axis relatively to the direction of motion (canting) have ρ_{HV} <1, suggesting depolarization. The same effect is observed for randomly oriented drops (black line), as the transmitted polarization has changed in the propagation through the medium.

The differential phase (δ_{HV}) refers to the phase difference between the horizontally and vertically polarized components of the received radar signal, providing valuable information about the shape and orientation of hydrometeors. In Fig. 3 right, very small diameters (D < 1 mm) are considered as spheres and present δ_{HV} = 0, indicating a consistent phase shift for both horizontal and vertical polarizations. As the diameter increases, δ_{HV} starts to show fluctuations. The canting angles introduce variability in the orientation of the drops within the radar beam, leading to variations in the observed δ_{HV}. Larger diameters exhibit more pronounced fluctuations due to the combined effects of canting and the transition from spherical to oblate shapes. When particles are randomly oriented (black line in Fig. 3 right), their orientations are distributed uniformly in all directions. In this case, the ensemble-averaged response over all possible orientations lead to cancellation effects in the differential phase (δ_{HV} =0). The cancellation occurs because, on average, the contributions from different orientations may have equal likelihood of positive and negative values, resulting in a net average of zero.

In Figure 4 we can see Linear Depolarization Ratio (LDR) and Differential Reflectivity (ZDR) simulations from T-matrix. LDR and ZDR measurements from a cloud radar provide valuable insights into the scattering properties of particles within clouds, including their shape, orientation, and composition.

LDR is a polarimetric radar parameter that quantifies the ratio of cross-polarized returns to co-polarized returns. It is often used to characterize the presence of non-spherical or partially oriented particles in the radar volume, such as ice crystals, aggregates, or horizontally oriented raindrops. Higher LDR values indicate stronger depolarization, which can be indicative of specific types of hydrometeors or particle orientations within clouds.

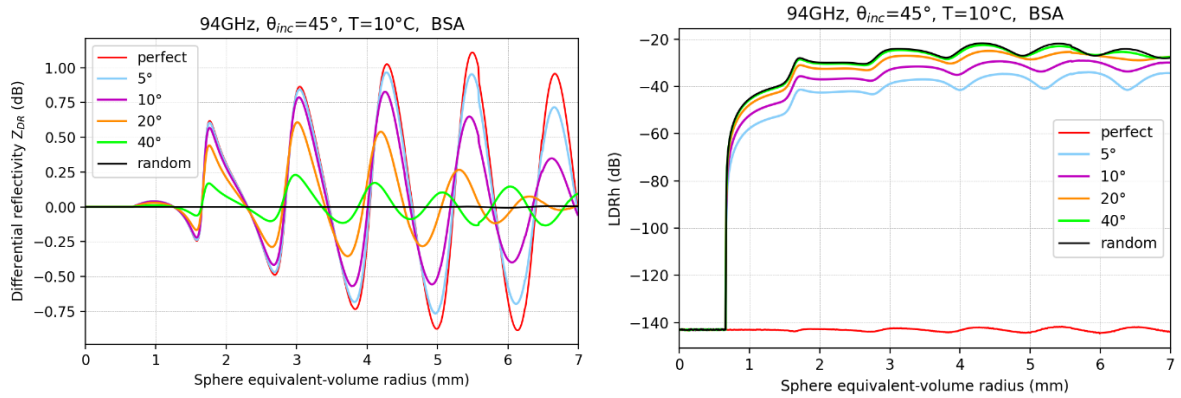

Figure 4 Differential reflectivity (Z_{DR}) and Linear Depolarization Ratio (LDR) as function of drops diameters for different orientation distribution functions.

The perfectly oriented particles (red line in Figure 4 right), do not depolarize and this is why we see LDR=140 dB. This is considered as minus infinity, because technically with a radar we will not be able to measure anything under -30dB. The same thing happens for small particles (D<0.7mm), as they are conceived as perfect spheres.

Why perfectly spherical particles do not depolarize?

Depolarization occurs when there is a change in the polarization state of the radar signal after interaction with scattering particles. In the case of perfect spheres, the radar signal will maintain its original polarization state (either horizontal or vertical) upon interaction with the spherical particles, and thus, there will be no depolarization.

ZDR is a polarimetric radar parameter that quantifies the difference in reflectivity between the H and V polarizations of the radar signal. providing information about the shape and orientation of scattering particles, as well as their composition and size distribution.

Positive ZDR values: the reflectivity is higher in the H polarization compared to the V polarization.
Negative ZDR values: the reflectivity is higher in the V polarization compared to the H polarization.

In Figure 4 left, we see that as we increase the canting, we see reduction of Zdr. The more the wobbling, the less the variability in Zdr.

FSA

Some forward scattering parameters we study are Differential Phase Shift (Kdp) and specific attenuation (A).

Specific Attenuation (A):

A is a measure of the attenuation or loss of radar signal power as it propagates through precipitation or cloud particles. A is related to the exponential decay of radar signal power with distance due to scattering and absorption by hydrometeors. A is also directly related to the integral of the DSD, particularly the intercept parameter of the DSD curve. A higher intercept parameter leads to a higher A value.

UNITS of Attenuation

20dB attenuation is a ratio. It means that the reflectivity is reduced by 20dB which in linear units means that reflectivity is reduced by a factor of 100. You start with dBZ, you subtract dB and you end up with dBZ.

10 dB → factor of 10
3 dB → factor of 2
6 dB → factor of 4
20 dB → factor of 100
30 dB → factor of 1000

$$B_{h\ or\ v} = 4.343 * \sigma_{eh\ or\ ev}$$

4.343 is the attenuation in dB and σ is the extinction cross section in m^2, so B_h is in $dB*m^2$.

$$A_h = \int B_h * N(D)dD$$

N(D) is in m^{-4}, B_h is in $dB*m^2$ and dD is in m, so the result will be in dB/m.

Differential Phase Shift (Kdp):

Kdp is a measure of the differential phase shift of the radar signal as it propagates through a medium. The differential phase shift is caused by the difference in propagation speeds of the horizontally and vertically polarized components of the radar signal due to scattering by hydrometeors. Kdp is directly related to the integral of the DSD, particularly the slope of the DSD curve. A steeper DSD slope leads to a higher Kdp value.

$$k = \frac{180}{\pi} * \lambda * Re\{S_{11} - S_{00}\}$$

$$Kdp = \int k * N(D)dD$$

Kdp is negative for the 94GHz and this is something extraordinary (Figure 5 left). If we produce the same for C band, it is positive and it is increasing with the size of the particles. For oblate spheroids we expect in Rayleigh region that the horizontally polarized radiation is attenuating more than the vertically polarized radiation and also is traveling with lower speed. Therefore, the Kdp come out positive because it expresses the phase shift introduced by the fact that when the wave is propagating inside these particles, the velocity of propagation of the horizontal wave is different from the velocity of the vertical. This wave propagates with two different velocities across a certain medium. Then this means that this medium will introduce a phase shift.

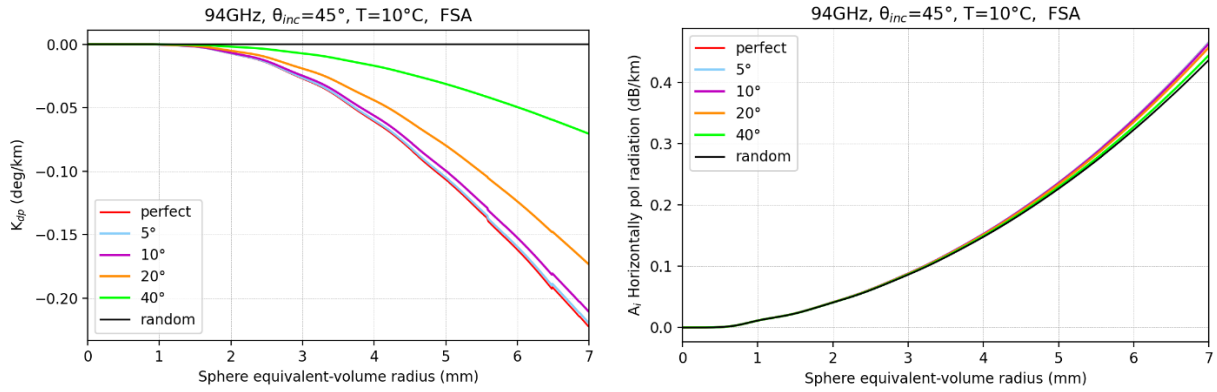

Figure 5 specific differential phase (K_{DP}) and Specific attenuation coefficient (A_i) as function of drops diameters for different orientation distribution functions.

Difference between the scattering differential phase δ_{hv} (BSA) and the specific differential phase K_{DP} (FSA).

The delta_hv is a phase shoft measured in degrees. This is something that happens in BSC. Once the wave impinges the particles, changes the phase and comes back.

The K_{DP} is a propagation effect. The EM has two components: a vertically and a horizontally polarized component. The specific differential phase K_{DP} tells you how the phase of the vertical wave and the phase of the horizontal wave changes as you go across. For example, if it is 10degrees/km, this means that after 10 km, the horizontal and the vertical wave will have a phase shift of 10 degrees.

In order to measure this, we need to receive in both channels. Simultaneous transmission and receiving mode, is usually found in RPG radar. In this case we are not able to derive LDR. In a radar system, we cannot measure all parameters. Some of them are mixed in the signal. So, we may be able to retrieve them but note that we don't directly measure them.

Single Scattering Calculation for a distribution of raindrops

The important thing is to separate propagation effects from backscattering effects using spectral analysis.

The fundamental idea is that the particles that are small, typically are not affected by backscattering effects. For instance, the δ_{hv} for BSC is zero for small particles. Same for Z_{DR}. So, if you look at the bit of the spectrum where we know there are small particles, there we will only see propagation effects. These small particles can be used as tracers for propagation effects only.

These Rayleigh targets (that we can identify) are used as tracers for attenuation effects.

We implement different drop size distributions (Gamma model) to the variables of interest, that are Z_{DR} and δ_{hv} for 2 different wavelengths according to the formulas:

$$\Delta_v = \int \delta_v(D)\sigma_v(D) \cdot [\exp(-\Lambda D) \cdot D^{\mu} dD] / \int \sigma_v(D) \cdot [\exp(-\Lambda D) \cdot D^{\mu} dD]$$

$$\Delta_h = \int \delta_h(D)\sigma_h(D) \cdot [\exp(-\Lambda D) \cdot D^{\mu} dD] / \int \sigma_h(D) \cdot [\exp(-\Lambda D) \cdot D^{\mu} dD]$$

$$\delta_{co} = \Delta_h - \Delta_v$$

$$Zdr = \int \sigma_h * N(D) dD / \int \sigma_v * N(D) dD$$

According to the results, we can reproduce simulations of the spectral polarimetric variables by using different gamma distributions that match better to the conditions we try to represent. More about this will be discussed at section 3.

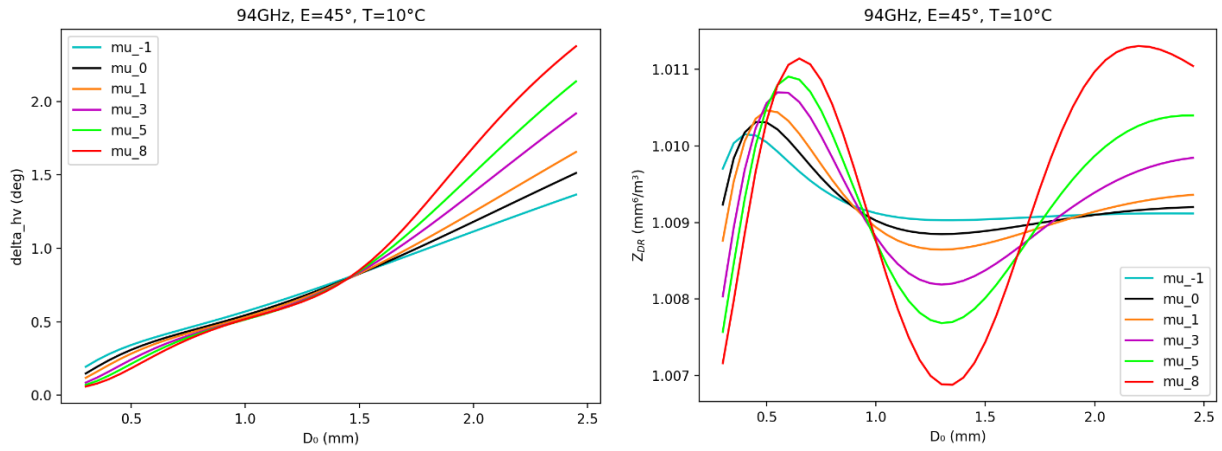

Figure 6 Scattering differential phase (delta_hv) and differential reflectivity (Z_{DR}) as a function of median volume diameter D_0 for different Gamma distribution parameters.

These plots are reproduced with D_0 on the x-axis, that defines the shape of the distribution (along with μ and N_0 also).

Comparison with real Data

Cloud radar systems are often equipped with Doppler capabilities, allowing them to measure the velocity of scattering particles within the radar's observation volume. This velocity information is crucial for studying the dynamics and microphysics of clouds and precipitation.

So, we perform a transition from the diameter space to the velocity space, hereafter spectral domain.

The relationship between the drops diameters and the corresponding velocities is a combination of cloud, drizzle and rain particles depending on the diameter.

$$V_{cloud} = 1.2 \cdot 10^{8} \cdot \left(\frac{D}{2}\right)^{2}$$

$$V_{drizzle} = 8333 \cdot \frac{D}{2} - 0.0833$$

$$V_{rain} = 9.65 - 10.3 \cdot e^{-0.6 \cdot 10^{3} \cdot D}$$

D is the diameter of the particle in meters.

After that, we can interpret the above-mentioned plots but now in spectral domain:

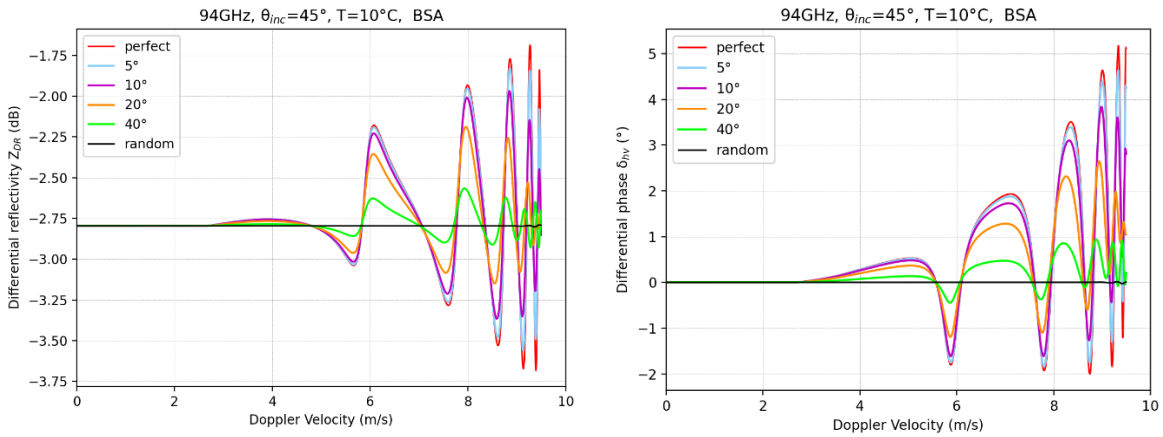

Figure 7 Co-polar correlation coefficient (rho_hv) and scattering differential phase as function of Doppler Velocties for different orientation distribution functions

Of course, if the vertical points at 45 degrees, we have to use the projection of the velocity, so multiply the velocity array with cos45°.

In other words, when we have a slant radar, we measure the components of vertical and horizontal droplet velocity of the measured velocity that is along the line of sight of the radar.

The overall purpose is to create a simulation tool in order to produce the theoretical spectral polarimetric variables that succesfully represent the real measurements. One example is presented below:

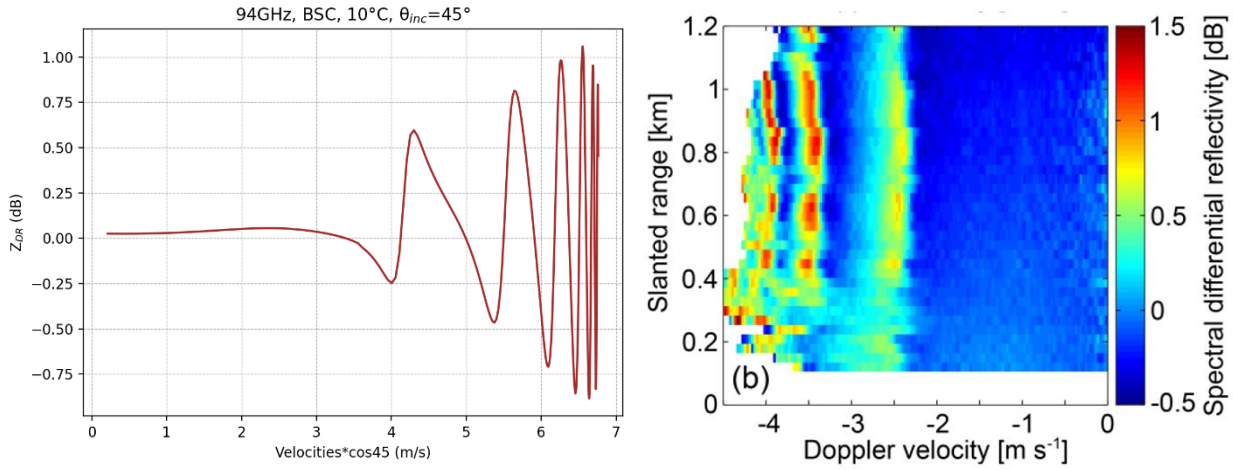

Figure 8 Spectral differential Reflectivity. Left: the simulated Z_{DR} line of the cross-section at a specific altitude. Right: Real data of a radar looking slant. (Myagov et al., 2020)

On the left part we see the simulation of Z_{DR} for a specific altitude in relationship to the slanted velocity. The peaks and valleys observed on the data (right part), are also observed in the simulation. The correspondence to different velocities accounts for the effect of wind, shifting the spectrum on the x-axis.

Simulations without noise and turbulence

The ideal Doppler Spectrum is a theoretical spectrum that is not contaminated by turbulence or noise. The equation for Doppler Spectrum is given by

$$\mathcal{S}_V(D) = \frac{\lambda^4}{\pi^5 \mid K^2 \mid} N(D)\sigma_{VV}(D)\frac{dD}{dv} \qquad [\frac{mm^6 m^{-3}}{ms^{-1}}]$$

where λ [mm] is the radar wavelength, $|K^2|$ is the dielectric factor of water, N (D) [$mm^{-1}m^{-3}$] is the DSD, σ_{VV} [mm^2] is the backscattering cross section for V channel and v[m/s] denotes the Doppler velocities of the drops. The spectrum from the V-channel is found below, in linear (left) and log (right) scale.

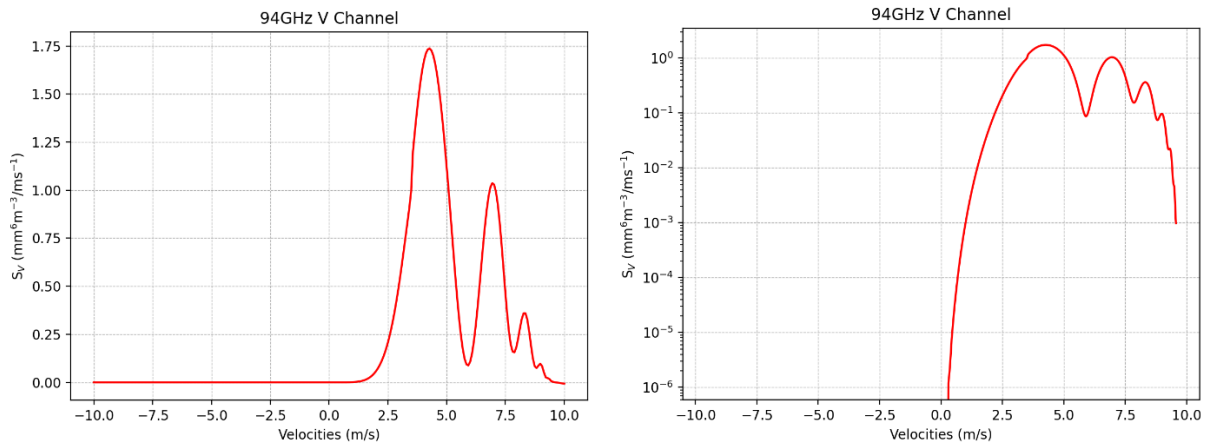

Figure 9 Simulated radar Doppler Spectrum S_V (mm^6m^{-3}/ms^{-1}) in linear and log scale. The integral of S_V along the velocities, gives the power of the spectrum in mm^6m^{-3}.

If we use different characteristics of the Gamma distribution, we can fit better a real data spectrum (black line in Figure 10)

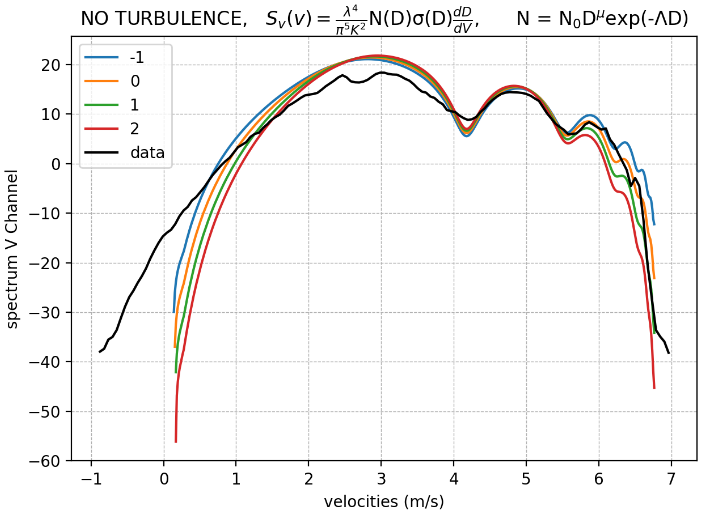

Figure 10 Example of a real data Spectrum (black line) and simulated spectrums with using distributions N(D) of different mu values.

Simulations with noise

In order to include noise in the simulations we apply the methodology by Yu et al., 2012.

The spectrum S_V is mapped into the velocity domain and sampled in correspondence to the envisaged Doppler velocity resolution and Nyquist interval at v_j with j = 1, 2, ..., N_{FFT} where N_{FFT} is the number of FFT points. The samples are indicated with S_V (v_j). Similarly, H-channel spectrum can also be produced at each velocity bin.

The time series of the V = I+iQ complex voltage signal in the V channel in the spectral domain can be written as:

$$\mathcal{V}_{V,k}^{[1]}(v_j) = \sqrt{-\mathcal{S}_V(v_j)\ln u_j^{[1]}}\; e^{i\theta_j^{[1]}} \qquad\qquad j = 1,\ 2,\ \ldots,\ N_{FFT}$$

where u and θ are independent, identically distributed random variables with uniform distribution between 0 and 1 and between -π and π, respectively. For the H channel in the spectral domain:

$$\mathcal{V}_{H,k}(k, v_j) = \sqrt{sZ_{DR}(v_j)}\left[s\rho_{HV}(v_j)\mathcal{V}_{V,k}^{[1]}(v_j) + \sqrt{1 - s\rho_{HV}{}^2(v_j)}\,\mathcal{V}_{V,k}^{[2]}(v_j)\right] e^{i s\delta_{HV}(v_j)}$$
$$j = 1,\ 2,\ \ldots,\ N_{FFT}$$

where the spectral variables $s\rho_{HV}$, $s\delta_{HV}$ and sZ_{DR} are generated as described in section 2, but also hold a character of s in the notation to differentiate from the commonly used polarimetric variables (Figure 11), and $V_{V,k}^{[2]}$ is generated according like $V_{V,k}^{[1]}$ with the same model spectrum $S_V(v)$, but with a second independent sequence of random numbers ($u^{[2]}$ and $\theta^{[2]}$). $s\rho_{HV}$, $s\delta_{HV}$ and sZ_{DR} are presented in the next Figure.

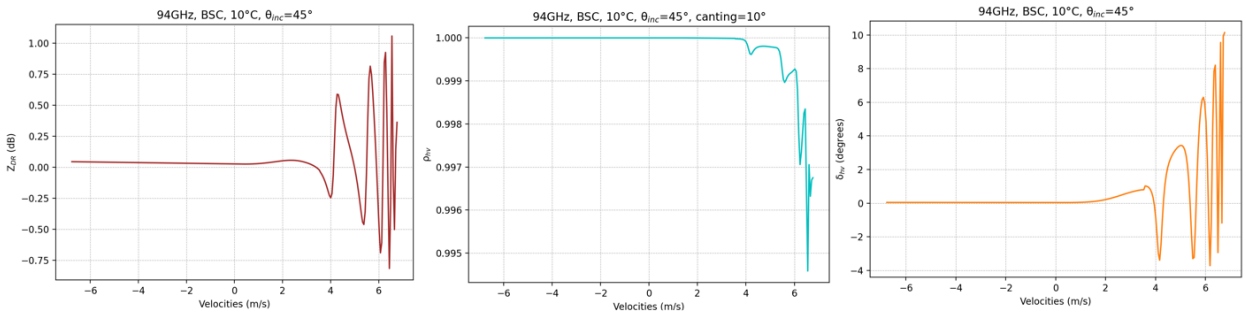

Figure 11 Spectral variables sp_{HV}, $s\delta_{HV}$ and sZ_{DR} as a function of Doppler Velocities.

This process is repeated for each velocity bin for a total of N_{FFT} spectral points within the Nyquist interval. The inverse Fourier transform of VV and VH are the simulated time series of complex signals for the V and H channels. For the implementation of white noise, we use similar equations:

$$\mathcal{N}_{V,k}(v_j) = \sqrt{-N_V \ln u_j^{[3]}}\; e^{i\theta_j^{[3]}}$$
$$\mathcal{N}_{H,k}(v_j) = \sqrt{-N_H \ln u_j^{[4]}}\; e^{i\theta_j^{[4]}}$$

where N_V and N_H are the noise level values for the V and H channel, and u, θ are again generated independently. Note that $N_{V,k}$ and $N_{H,k}$ are also complex numbers.

The complex numbers that represent the simulation of the noisy Doppler spectrum for V and H channel are calculated from:

$$S_{VV,k}(v_j) = \mathcal{V}_{V,k}(v_j) + \mathcal{N}_{V,k}(v_j)$$
$$S_{HH,k}(v_j) = \mathcal{V}_{H,k}(v_j) + \mathcal{N}_{H,k}(v_j) \qquad j = 1,\ 2,\ \ldots,\ N_{FFT}$$

The SvvSvv* will be the Doppler Spectrum Amplitude:

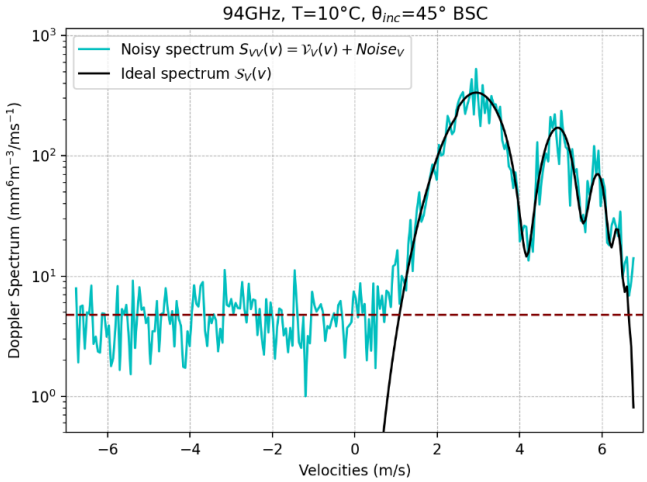

Figure 12 Simulated Radar Spectrum: without noise (black line) and with noise (blue line).

In Figure 12, the dark red line represents the noise level (white noise), the black line is the ideal spectrum as in Figure 9 and the blue line is the noisy spectrum.

In order to acquire the spectral polarimetric variables we use the formula:

$$\rho_{HV} e^{i\delta_{HV}} = \frac{S_{HH} S^{\star}_{VV}}{\sqrt{|S_{HH}|^2 |S_{VV}|^2}}$$

The amplitude will be the copolar correlation coefficient ρ_{hv} and the phase will be the scattering differential phase δ_{hv} with the effect of noise (Figure 13).

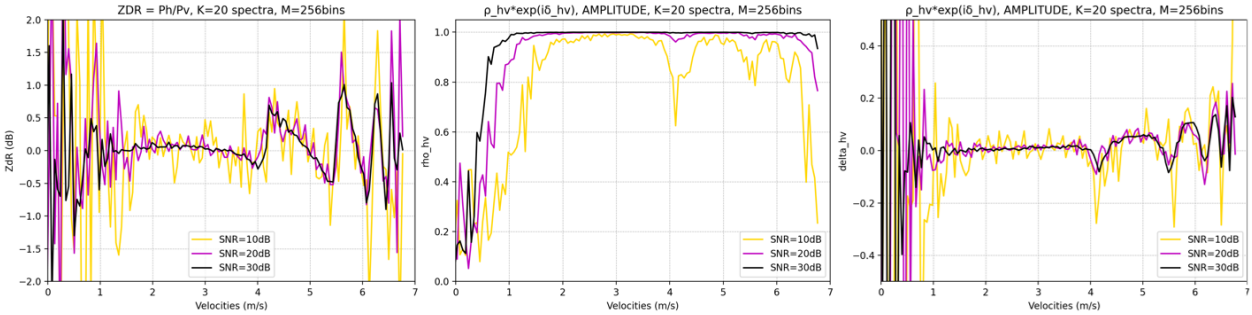

Figure 13 Spectral variables $s\rho_{HV}$, $s\delta_{HV}$ and sZ_{DR} as a function of Doppler Velocities, simulated for different SNR.

The different lines represent simulations with different SNR values. SNR is used as input to produce the noise levels for the V and H channel N_V and N_H in the $N_{V,k}$ and $N_{H,k}$ formula as described earlier in this Chapter.

Simulations with noise and turbulence

Understanding the effects of turbulence on the Doppler spectrum is crucial for improving the accuracy of radar observations and their interpretation.

Atmospheric turbulence causes random fluctuations in the velocity of hydrometeors. As a result, the Doppler spectrum broadens, because the turbulent motion introduces a range of velocity com ponents, contributing to a spread of Doppler shifts in the radar return.

To introduce the turbulent motions of drops in the simulations, each element Zij of the Z matrix is con volved with a turbulence term Sair. The convolution operation, denoted here as *, is mathematically expressed as:

$$(Z_{ij} * S_{\text{air}})(v) = \int_{-\infty}^{\infty} Z_{ij}(v - \xi) \cdot S_{\text{air}}(\xi)\, d\xi$$

where ξ is the convolution variable and Sair incorporates the turbulent motions of drops within the atmosphere:

$$S_{air}(v) = \frac{1}{\sqrt{2\pi}\sigma_t} \cdot e^{-\frac{v^2}{2\sigma_t^2}}$$

with σ_t[m/s] expressing the turbulence broadening of the Doppler spectrum. S_{air} is a Gaussian function that obtains different shape depending on the σ_t value.

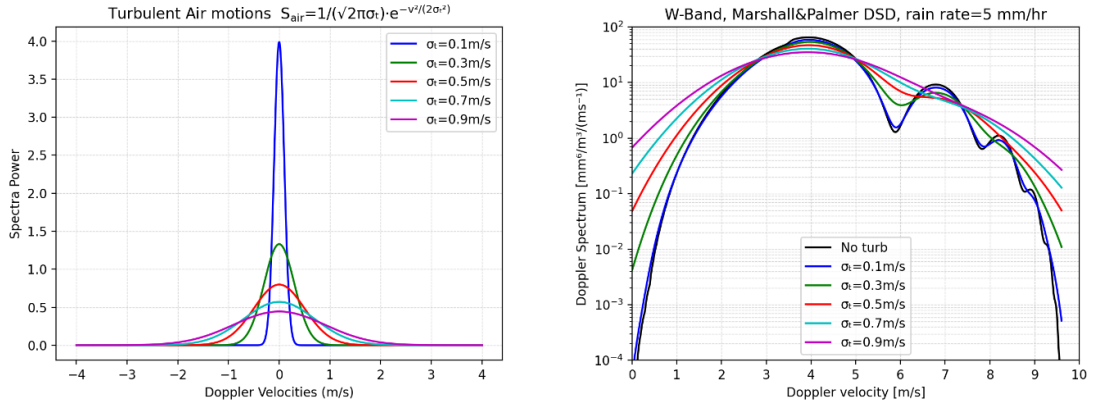

Figure 14 Left: Spectra power of turbulent motions. Right: Doppler Spectrum for different turbulent conditions.

Subsequently, in order to include the turbulence effect, we recalculate $s\rho_{HV}$, $s\delta_{HV}$ and sZ_{DR} by using the convolved Z_{ij} and then apply equations of S_{vv} and S_{hh}. The modeled spectrum S_V is also convolved with the turbulence term. This way, the time series of complex signals from both channels include the effect of turbulence. In the final step, we calculate the com plex numbers that represent the simulation of the real Doppler spectrum for V and H channel and the spectral polarimetric variables.

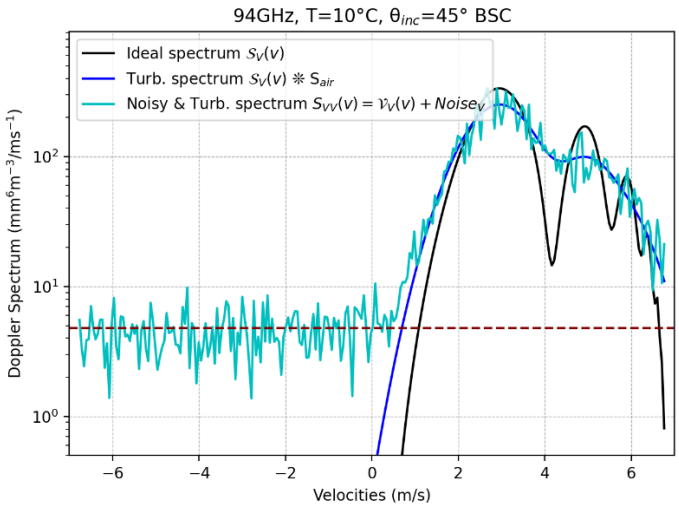

Figure 15 Simulated Radar Spectrum: without noise and turbulence (black line), with turbulence (dark blue) and with noise and turbulence (light blue line).

Similarly with Figure 12, the dark red line in Figure 15 is the noise level, the black line is the ideal spectrum without turbulence or noise, the dark blue line is the turbulent spectrum and the light blue line is the noisy and turbulent spectrum.

The following figure provide a visual representation of the simulated spectral polarimetric variables. These simulations account for the turbulent motions inherent in the atmosphere.

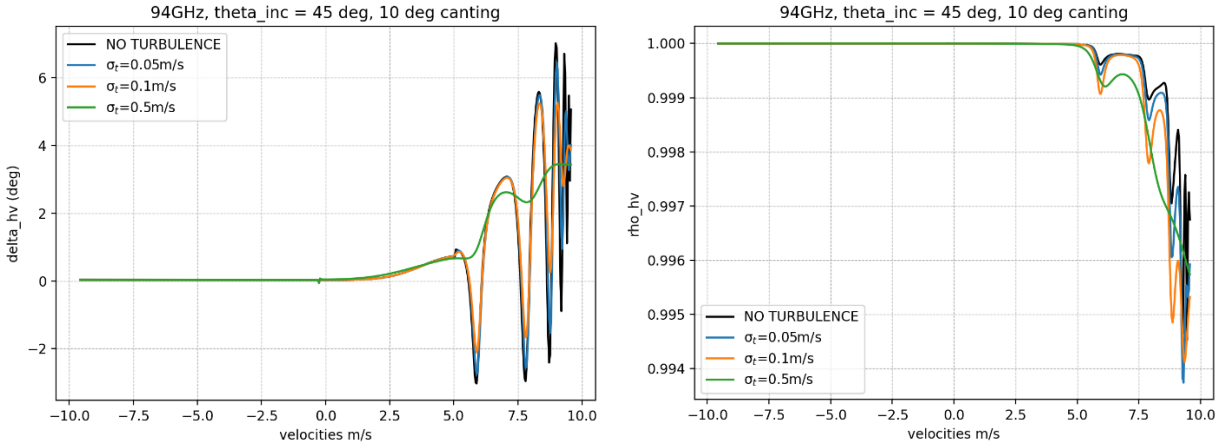

Figure 16 Spectral variables sp_{HV}, $s\delta_{HV}$ and sZ_{DR} as a function of Doppler Velocities, simulated for different turbulent conditions.

4 References

- Mishchenko, Michael I., Joachim W. Hovenier, and Larry D. Travis, eds. Light scattering by nonspherical particles: theory, measurements, and applications. Elsevier, 1999.

- Testud, Jacques, et al. "The concept of "normalized" distribution to describe raindrop spectra: A tool for cloud physics and cloud remote sensing." Journal of Applied Meteorology and Climatology 40.6 (2001): 1118-1140. [link]

- Leinonen, Jussi. "High-level interface to T-matrix scattering calculations: architecture, capabilities and limitations." Optics express 22.2 (2014): 1655-1660. [link]

- https://github.com/jleinonen/pytmatrix/wiki

- Lhermitte, Roger. "Attenuation and scattering of millimeter wavelength radiation by clouds and precipitation." Journal of Atmospheric and Oceanic Technology 7.3 (1990): 464-479. [link]

- Fabry, Frédéric. Radar meteorology: principles and practice. Cambridge University Press, 2018.

- Tridon, Frédéric, Alessandro Battaglia, and Pavlos Kollias. "Disentangling Mie and attenuation effects in rain using a Ka-W dual-wavelength Doppler spectral ratio technique." Geophysical Research Letters 40.20 (2013): 5548-5552. [link]

- Myagkov, Alexander, Stefan Kneifel, and Thomas Rose. "Evaluation of the reflectivity calibration of W-band radars based on observations in rain." Atmospheric Measurement Techniques 13.11 (2020): 5799-5825. [link]

- Mallet, Cécile, and Laurent Barthes. "Estimation of gamma raindrop size distribution parameters: Statistical fluctuations and estimation errors." Journal of Atmospheric and Oceanic Technology 26.8 (2009): 1572-1584. [link]

- Yu, Tian-You, Xiao Xiao, and Yadong Wang. "Statistical quality of spectral polarimetric variables for weather radar." Journal of Atmospheric and Oceanic Technology 29.9 (2012): 1221-1235. [link]

- Zhu, Zeen, Pavlos Kollias, and Fan Yang. "Particle inertial effects on radar Doppler spectra simulation." Atmospheric Measurement Techniques 16.15 (2023): 3727-3737. [link]